ACS APPLIED MATERIALS & INTERFACES

Research Article

Cite This: ACS Appl. Mater. Interfaces 2018, 10, 8307−8316

www.acsami.org

Polydopamine-Coated Main-Chain Liquid Crystal Elastomer as Optically Driven Artificial Muscle

Hongmiao Tian,[†,‡,#] Zhijian Wang,[‡,#] Yilong Chen,[‡] Jinyou Shao,[†] Tong Gao,[∥,⊥] and Shengqiang Cai*[,‡,§]

[†]Micro- and Nano-technology Research Center, State Key Laboratory for Manufacturing Systems Engineering, Xi'an Jiaotong University, 28 Xianning Road, Xi'an 710049, P. R. China

[‡]Department of Mechanical and Aerospace Engineering and [§]Materials Science and Engineering Program, University of California, San Diego, La Jolla, California 92093, United States

[∥]Department of Mechanical Engineering and [⊥]Department of Computational Mathematics, Science and Engineering, Michigan State University, East Lansing, Michigan 48824, United States

Supporting Information

ABSTRACT: Optically driven active materials have received much attention because their deformation and motion can be controlled remotely, instantly, and precisely in a contactless way. In this study, we investigated an optically actuated elastomer with rapid response: polydopamine (PDA)-coated liquid crystal elastomer (LCE). Because of the photothermal effect of PDA coating and thermal responsiveness of LCE, the elastomer film contracted significantly with near-infrared (NIR) irradiation. With a fixed strain, light-induced actuating stress in the film could be as large as 1.5 MPa, significantly higher than the maximum stress generated by most mammalian skeletal muscle (0.35 MPa). The PDA-coated LCE films could also bend or roll up by surface scanning of an NIR laser. The response time of the film to light exposure could be as short as 1/10 of a second, comparable to or even faster than that of mammalian skeletal muscle. Using the PDA-coated LCE film, we designed and fabricated a prototype of robotic swimmer that was able to swim near the water−air interface by performing "swimming strokes" through reversible bending and unbending motions induced and controlled by an NIR laser. The results presented in this study clearly demonstrated that PDA-coated LCE is a promising optically driven artificial muscle, which may have great potential for applications of soft robotics and optomechanical coupling devices.

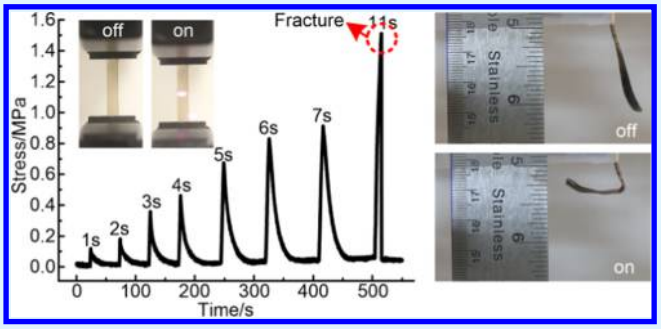

KEYWORDS: *artificial muscle, optically driven actuators, soft robots, liquid crystal elastomer, polydopamine*

1. INTRODUCTION

Soft active materials which can undergo reversible shape or volume change under external stimuli, such as electricity,[1,2] magnetism,[3,4] heat,[5,6] chemistry,[7,8] light,[9,10] and gas,[11,12] have attracted increasing attention for their applications in soft robotics,[13,14] artificial muscle,[15,16] cell capture and release,[17,18] and so on. Among these stimuli, light is a clean energy source that can be controlled remotely, instantly, and precisely without physical contact. Optically driven actuators have been extensively explored in designing a myriad of devices and structures, showing the capability of converting optical energy into mechanical work.[19−21] Diverse modes of deformation and motion, including contraction,[22] expansion,[23] bending,[24] twisting,[25] and oscillation,[26] have been achieved in optically responsive materials. For instance, Lubineau et al. fabricated single-walled carbon nanotube (SWCNT) and poly(vinylidene fluoride) bilayer structure to realize optically controlled spring and soft grippers.[27] Pisano et al. reported a polycarbonate/SWCNT bilayer structure, which could bend about 90° when turning on the light and revert back to the relaxed state when turning off. This material has been further explored to fabricate forward-moving motor driven by directional light illumination.[28]

Recently, a variety of photomechanical coupling polymers have been reported, including optically responsive hydrogels,[29,30] shape memory polymers (SMPs),[31,32] and liquid crystal elastomers (LCEs).[33,34] For example, Asher et al. demonstrated a UV-responsive hydrogel by integrating photoisomerizable azobenzene functional groups into polymer chain.[35] Another way of making photomechanical coupling hydrogels is through mixing photothermal particles into thermally responsive hydrogels.[36−39] For instance, Hayward et al. designed waveguiding microactuators based on photoresponsive nanocomposite hydrogel.[40] However, responsive

Received: January 12, 2018
Accepted: February 15, 2018
Published: February 15, 2018

DOI: 10.1021/acsami.8b00639
ACS Appl. Mater. Interfaces 2018, 10, 8307−8316

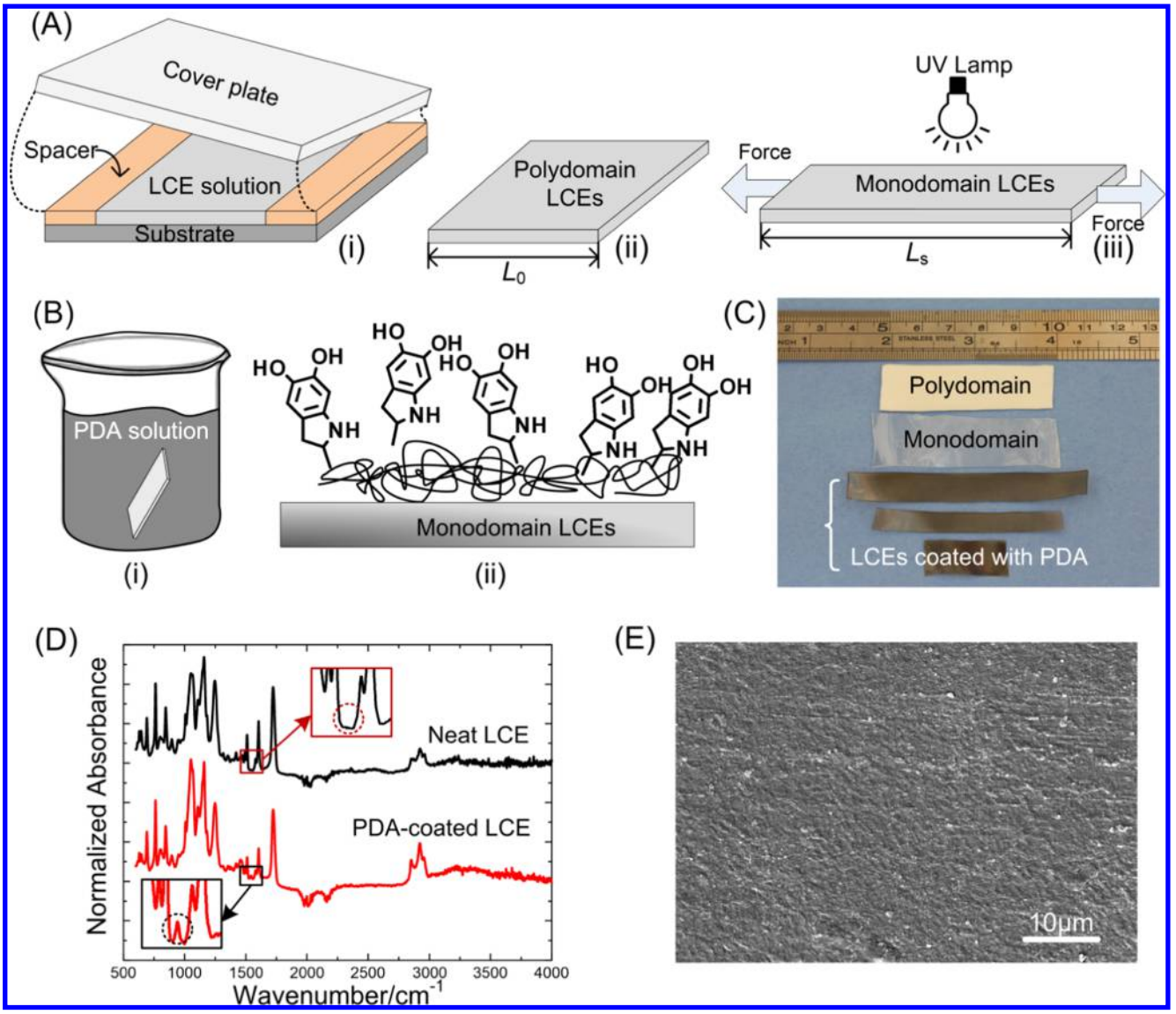

Figure 1. Fabrication and characterization of (A) monodomain liquid crystal elastomers (LCEs) and (B) polydopamine (PDA)-coated monodomain LCEs using dip-coating process. (C) Polydomain, monodomain, and PDA-coated monodomain LCE samples. (D) Fourier transform infrared (FTIR) spectra for neat LCE film and PDA-coated LCE film. (E) Scanning electron microscopy (SEM) image of PDA-coated LCE film after multiple actuation tests.

hydrogels usually can only work in water, and the response of gels is usually slow because of the involvement of solvent diffusion. SMPs have also been employed as photomechanical coupling materials.[41,42] However, most SMP-based structures cannot switch their configurations reversibly for a large number of cycles. Therefore, it is still very challenging to develop useful structures based on optically responsive soft materials.

LCEs have been explored widely for applications as soft artificial muscles because of their large and reversible deformation induced by various stimuli. LCE is known as a combination of liquid crystal molecules and flexible polymer chains, exhibiting a fast and reversible response under thermal stimuli. Monodomain LCEs in which the liquid crystal molecules align uniformly can show dramatic reversible deformation via crystalline−isotropic phase transition upon heating up or cooling. When the temperature is above the phase-transition temperature, aligned liquid crystal molecules become randomly oriented, which induces macroscopic contraction of LCE along the direction of alignment. On the contrary, when the temperature is reduced, randomly oriented liquid crystal molecules become aligned in one direction, which induces macroscopic expansion of LCE along the direction of alignment.

Similar to other responsive materials discussed above, two methods have also been adopted to make LCE responsive to light: the first one is through introducing photoresponsive liquid crystal molecules like azobenzene chromophores into LCE. The azobenzene chromophores can transit from trans to cis configuration under UV light exposure because of the photoisomerization, which consequently induces reversible deformation of the polymer.[43−47] For example, Huang et al. fabricated a microsoft swimming robot using a polymer film containing azobenzene chromophores. Periodically flashing UV light and white light drove the flagellum of the robot to swing periodically for moving forward in water.[48] However, the need for dual-wavelength operation (UV and visible) for reversible actuation may constrain the applications of LCEs in some senarios.[28] The other approach is through incorporating light-

DOI: 10.1021/acsami.8b00639
ACS Appl. Mater. Interfaces 2018, 10, 8307−8316

absorbing fillers like carbon nanotubes and graphene into LCE matrix.[10,49] For example, Keller et al. fabricated light-driven LCE microactuators by incorporating gold nanospheres and nanorods into the elastomer.[50,51] However, the incorporation of various fillers can dramatically change the mechanical properties of LCE and also affect its actuation behavior, which makes the performance of LCE actuators less controllable. These limitations motivated us to fabricate a light-responsive LCE with fast response, as well as large actuating stress and strain, which can also be easily manufactured into various sizes and shapes.

Recently, a new kind of photothermal material, polydopamine (PDA), has been widely explored due to its excellent photostability as well as strong absorption in the near-infrared (NIR) region. It is reported that the molar extinction coefficient of PDA nanoparticles at the light irradiation of 808 nm wavelength is 100 times higher than that of CNTs.[52,53] Ji et al. explored doping and coating methods of PDA into shape memory polymer to make NIR-responsive materials with a response time of roughly 15 s.[53,54] As a composition of adhesive proteins in mussels, dopamine can undergo a self-polymerization process and form a thin and surface-adherent PDA layer on multifarious materials, as reported by Messersmith et al.[55] Frick et al. utilized an adherent PDA coating as a binder layer to deposit a conductive metallic layer onto the surface of LCE. No delamination was detected in the sample during a large number of thermal actuation cycles.[56] The excellent photothermal effect and strong adhesive property of PDA and its composites uncovered in different experiments inspire us to develop optically driven active structures based on PDA-coated LCEs.

In this study, we fabricated an optically responsive elastomer film based on PDA-coated main-chain LCE, which could work in both air and water. The fabrication process of PDA-coated LCE films is very simple and versatile, which only involves molding, prestretch, and dip-coating process. The film could generate large actuating stress in response to NIR irradiation. Additionally, PDA-coated LCE films could bend dramatically within a second when exposed to a laser point, which exhibits a much faster response than most previously fabricated LCEs with large deformation. An artificial fish, based on PDA-coated LCE film, was designed and fabricated, which could swim on the surface of water under NIR irradiation. The fabrication process of PDA-coated LCE film proposed in the article may be useful in developing optically driven artificial muscle and soft robots.

2. MATERIALS AND METHODS

2.1. Materials. (1,4-Bis-[4-(3-acryloyloxypropyloxy)benzoyloxy]-2-methylbenzene) (RM257, 95%, Wilshire Technologies), (2-hydroxyethoxy)-2-methylpropiophenone (HHMP, 98%, Sigma-Aldrich), 2,2′-(ethylenedioxy)diethanethiol (EDDET, 95%, Sigma-Aldrich), pentaerythritol tetrakis(3-mercaptopropionate) (PETMP, 95%, Sigma-Aldrich), dipropylamine (DPA, 98%, Sigma-Aldrich), VHB film (3 M company), dopamine hydrochloride (99%, Alfa Aesar), and Tris base (Fisher Scientific) were used as received without further purification.

2.2. Fabrication of Main-Chain LCE Films. The LCE film was prepared following the procedures reported by Yakacki et al.[57,58] RM257 (12.00 g, 20.39 mmol), the diacrylate mesogen, was dissolved in toluene, and the mixture was heated at 85 °C to form a homogeneous solution. Then, 0.0772 g of HHMP (0.34 mmol) as the photoinitiator for cross-linking reaction in the second polymerization stage was added into the solution and heated to be dissolved. After that, 2.7360 g of EDDET (15.01 mmol), which acts as flexible spacer in LCE, and 0.6996 g of PETMP (1.43 mmol), the tetra-arm thiol cross-linker, were added into the stirring RM257 solution dropwise. The Michael addition reaction catalyst (0.0378 g of DPA (0.37 mmol)) was added later. The mixture was degassed in vacuum to remove the bubbles inside and filled into a rectangular glass mold with the thickness of 1 mm. The reaction proceeded at room temperature overnight and then the loosely cross-linked film was put into a convection oven at 85 °C for 6 h to evaporate the toluene. When cooled to the ambient temperature, the LCE film appeared opaque, indicating that it was in polydomain state. In subsequent step, the polydomain film was uniaxially stretched and placed under 365 nm UV light (UVP high-intensity UV inspection lamp) for 15 min to complete the second cross-linking reaction to obtain a monodomain film. The UV light intensity was 16.7 mW/cm^2. Specifically, the photoinitiator (HHMP) could generate free radicals under UV light, which triggered the second-step cross-linking reaction to fix the LCE sample in monodomain state. A series of monodomain samples with various magnitudes of prestretch had been prepared. As shown in Figure 1A, the prestretch is defined as the ratio of the length L_s of the monodomain LCE films to the initial length L_o of the polydomain LCE films. In the current work, the cross-linking density of LCE was controlled by the excessive amount of acrylate groups on RM257 over the thiol groups on EDDET and PETMP. In our experiment, the excessive amount was 15 mol %. The cross-linking density of the LCE can be increased by increasing the excessive amount of acrylate groups.

2.3. Fabrication of PDA-Coated LCE Films. Dopamine hydrochloride (0.2 g, 1.05 mmol) and Tris base (0.1 g, 0.83 mmol) were dissolved in 100 mL of water. The pH value of the Tris base buffer solution was 8.5 measured by pH testing paper (HYDRION pH 1.0−11.0, Micro Essential Lab). The monodomain LCE films were immersed in the solution and stirred for 24 h. The pH value of the buffer solution kept the same. The resultant PDA-coated LCE films were washed with deionized water three times and air-dried.

2.4. Characterization of the PDA-Coated LCE Films. Fourier transform infrared spectra for neat LCE film and PDA-coated LCE film were obtained by Fourier transform infrared spectroscopy (FTIR, NICOLET iS10, Thermo Fisher Scientific). We saw similar FTIR results, obtained at different testing points of the same sample. The thickness of the PDA coating was measured by atomic force microscopy (AFM, INNOVA, Veeco). In the testing process, a tape was used as a physical mask to prevent the generation of PDA film, resulting in a film edge for measuring the thickness of the PDA film. The operation mode of AFM was tapping mode, and the thickness was estimated by point-to-point analysis as well as several testing for the average value. The surface morphology of the PDA-coated LCE film was examined by scanning electron microscopy (SEM, Hitachi SU8010, Japan). During the testing process, a Au film of about 5 nm thickness was deposited onto the sample surface to improve its electronic conductivity. The specifications for the SEM test were: accelerating voltage: 5.0 kV; working distance: 13.4 mm; and high chamber pressure. The differential scanning calorimetry (DSC) curve of the LCE film was obtained from DSC1 Mettler Toledo, Switzerland, with the heating/cooling rate of 20 °C/min. The temperature mapping of the PDA-coated LCE film was measured by FLIR T630. In the testing process, the sample size was roughly 5 mm (L) × 2.5 mm (w) × 1 mm (t).

2.5. Measurement of NIR Laser-Induced Actuating Stress in PDA-Coated LCE Films. To evaluate the light-induced actuating stress generated in the PDA-coated LCE film, 3 cm (L) × 0.7 cm (w) × 0.1 cm (t) cm flexible films were preloaded with 0.1 N force to keep the films taut using a uniaxial testing machine (Instron 5965 Dual Column Universal Testing System, Massachusetts). The load cell in the uniaxial testing machine was Instron 2712-042 with a capacity of 2 kN (Instron, Massachusetts). Then, NIR laser irradiation (SKY laser with a wavelength of 808 nm and power density of 3.1 W/cm^2) was applied in the middle of the specimen and the actuation stress was recorded by the load cell of the machine. The effect of irradiation duration on actuating stress was also studied.

2.6. NIR Laser-Induced Deformation of the PDA-Coated LCE Films. To study the deflection of PDA-coated LCE films, a cantilever

DOI: 10.1021/acsami.8b00639
ACS Appl. Mater. Interfaces 2018, 10, 8307−8316

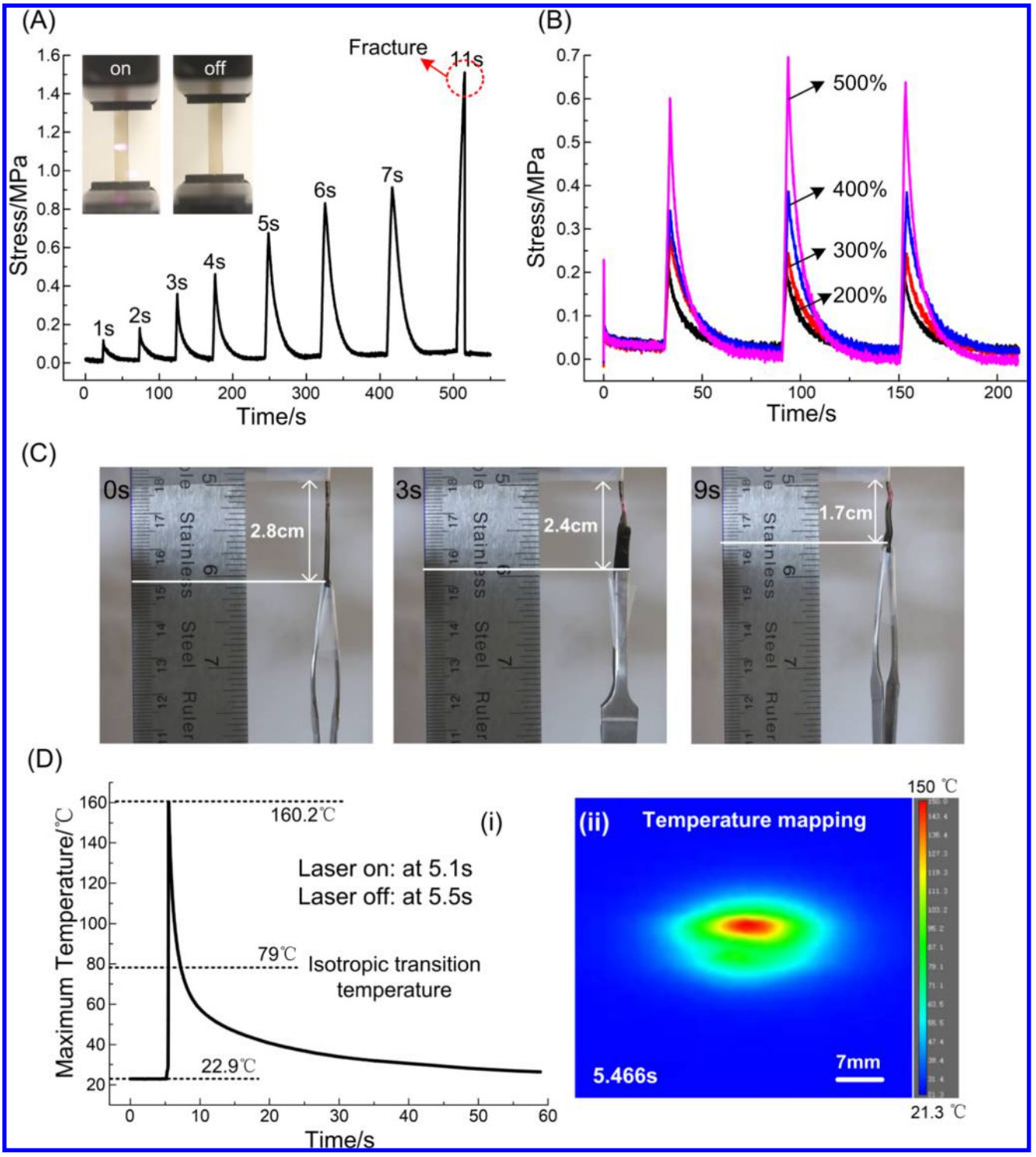

Figure 2. Influence of irradiation time (A) and prestretch (B) on the generated actuating stress in a PDA-coated monodomain LCE film. (C) Demonstration of a PDA-coated monodomain LCE film with a weight of 0.1 g lifting a pair of tweezers of 12 g, induced by NIR light irradiation. (D) The highest temperature in the film under the NIR laser irradiation as a function of time (i), and the temperature distribution in the film 0.366 s after the laser was turned on.

beam configuration was adopted in the experiments. Once the NIR laser irradiation was applied, the LCE strip bent immediately. A digital camera was used to record the dynamics of the bending of the PDA-coated LCE films in both air and water.

2.7. Fabrication of Artificial Fish. The body of the artificial fish was made up of VHB films with thickness of 1 mm using laser cutting (LaserCAMM) to mimic the two-dimensional shape of a fish. The PDA-coated LCE film with prestretch of 500% was tailored to the shape of fish tail. The two parts were glued together to obtain an entire soft fish.

3. RESULTS AND DISCUSSION

3.1. Design and Fabrication of PDA-Coated LCE Film.

Figure 1 schematically illustrates the fabrication process of monodomain LCEs coated by PDA. The process was facile and

DOI: 10.1021/acsami.8b00639
ACS Appl. Mater. Interfaces 2018, 10, 8307−8316

scalable, which only involved molding, prestretch, and dip coating. In detail, an LCE precursor solution was filled into a rectangular glass mold with a spacer thickness of 1 mm and covered by a flat glass plate as shown Figure 1A-i. Then, a polydomain LCE film was obtained after evaporating the solvent as shown in Figure 1A-ii. In a polydomain LCE, tiny nematic domains of mesogens randomly distributed. To achieve large actuating stress and strain, we need to synthesize LCE films in monodomain state. In the experiment, we applied a uniaxial tensile force to transfer the polydomain LCE film to monodomain state. The stretched LCE film was then exposed to UV light for further polymerization due to the excessive acrylate groups, as shown in Figure 1A-iii. In this process, the polydomain was synthesized in the isotropic state due to the presence of solvent, and the monodomain is cross-linked in the nematic state at room temperature. The glass-transition temperature (T_g) of the LCE is around 2 °C according to the DSC measurement, as shown in Figure S1-i in the Supporting Information. The mesogenic molecules in both polydomain and monodomain LCE were in nematic phase at room temperature. The isotropic transition temperature of the LCE was around 79 °C according to the DSC measurement, as shown in Figure S1-ii in the Supporting Information.

To make the LCE film optically responsive, the film was submerged into a dopamine/Tris base buffer solution. The surface of LCE film turned into gray after 24 h, indicating the formation of PDA layers on the LCE surface via the self-polymerization of dopamine, as illustrated in Figure 1B. The coating method was very repeatable and could be applied to LCE (and other polymers) of different sizes and shapes because of the excellent surface-adherent property of PDA. The size and shape of the PDA-coated LCE film can be easily controlled by using properly designed mold.

Figure 1C shows the photos of the polydomain, monodomain, and PDA-coated monodomain LCE films. The monodomain LCE film is transparent, and the PDA-coated LCE is black, which indicates its capability of absorbing light. When NIR laser irradiation is applied, the PDA layer can transform light into heat rapidly, leading to the increase of the temperature in LCE. Subsequently, the LCE film can contract due to nematic phase to isotropic phase transition in the elastomer.

The polymerized dopamine on the surface of the LCE film could also be clearly seen by comparing the FTIR spectra for neat LCE film and PDA-coated LCE film, which are given in Figure 1D. For the PDA-coated LCE film, a new peak between 1600 and 1650 cm^{-1} corresponding to the C−H out-of-plane bending of the benzenoid aromatic ring appeared, which was consistent with the report by Baginska et al.[59]

To measure the thickness of the coated PDA layer, we used a tape as a mask to cover part of the LCE film during the dip-coating process, resulting in an edge between the PDA-coated area and uncoated area, as shown in Figure S2. Using AFM, we conducted point-to-point analysis with the tapping mode and estimated the average thickness of the PDA coating to be around 51 nm with a standard deviation of 7 nm. The measured thickness was close to the one reported by Li et al. (~30 nm).[54] The difference may be attributed to the different absorption capacity of the polymer. The thickness of the LCE film was around 1 mm, which was much larger than that of the PDA coating. Thus, the effect of the thin PDA coating on the mechanical response of the LCE film was negligible, which was consistent with the results shown by Li et al.[54] In the experiment, we did not observe any wrinkles and cracks of the PDA coating after multiple actuation tests, as shown in the SEM image (Figure 1E).

3.2. Optically Induced Actuating Stress/Strain in a PDA-Coated LCE Film. To quantitatively measure the optically induced actuating stress and strain in PDA-coated LCE film, we conducted the tests as shown in the inset of Figure 2A. Both ends of the LCE film were fastened to the uniaxial testing machine, and a tensile force of 0.1 N was applied to the film to keep it taut. The actuating stress generated in the LCE could be recorded as a function of time, with laser irradiation being applied onto the middle part of the specimen. More details about the experiments can be found in Materials and Methods. When an NIR laser was exposed onto the LCE film, the surface PDA layer transformed the light into heat instantly. It was found in the experiment that the actuating stress generated in the film increased from zero immediately after the light was turned on. The magnitude of the actuating stress could be increased by increasing the irradiation time. For an irradiation time of 1 s, the magnitude of stress could be raised to 0.11 MPa, which was comparable to the magnitude of stress generated by sustainable mammalian skeletal muscle (≈0.1 MPa).[60] The response time was also comparable to that of mammalian skeletal muscle (roughly at 0.1−0.5 s).[61] When the irradiation time was increased to 3 s, the magnitude of the actuating stress could reach around 0.4 MPa, comparable to maximum stress generated by mammalian skeletal muscle (≈0.35 MPa).[60] When the irradiation time was further increased to 11 s, the magnitude of actuating stress could reach 1.5 MPa, much higher than that of the stress generated in mammalian skeletal muscle. The increase of irradiation time resulted in higher temperature and larger actuation stress. Further increasing the irradiation time could lead to the breakage of specimen, indicating that the actuating stress exceeded the strength of the material. It also shows the possibility to achieve an even higher actuating stress through enhancing the strength of the LCE film.

Another factor that can affect the actuating stress is the magnitude of the prestretch in the second cross-linking step of monodomain LCE film. Several monodomain LCE with various prestretches were prepared as described in Materials and Methods. Figure 2B illustrates the influence of the prestretch on the actuating stress with a fixed irradiation time of 3 s. For the same irradiation time, a higher stress could be achieved in the LCE film with larger prestretch. With a prestretch of 200%, the actuating stress was around 0.2 MPa, whereas the stress could be increased to 0.6 MPa with a prestretch of 500%. The increment was about 3 times by only adjusting the prestretch. Therefore, it is an effective approach to increase the maximum actuating stress of PDA-coated LCE films by applying a larger prestretch during the fabrication process. It is noted that the critical stretch for polydomain−monodomain transition of the LCE was roughly 2 (Figure S3), which was the lower bound of the investigated prestretches in Figure 2B.

It can be clearly seen from Figure 2A,B that actuation of the LCE was faster than its recovery. It is because the thermal transferring processes in the LCE were different for actuation and recovery. For the actuation, the LCE was heated up mainly through heat conduction, and the speed may mainly depend on the thermal conductivity of LCE. When the laser was turned on, the PDA coating converted light to heat almost instantly and became a heat source in contact with interior LCE. However, the cooling process was mainly through thermal

DOI: 10.1021/acsami.8b00639
ACS Appl. Mater. Interfaces 2018, 10, 8307−8316

convection and radiation, which is much slower due to the small heat transfer coefficient in the air.

Because of the high optically induced stress generated by the PDA-coated LCE film, it could be utilized as an artificial muscle to lift an object, as shown in Figure 2C. In the demonstration, we manually scanned an NIR laser spot on the surface of the PDA-coated LCE film from bottom to top to achieve uniform heating as well as homogeneous contraction. The scanning motion of the laser spot can be found in Movies S1 and S2 in the Supporting Information. Before the laser scanning, the length of the PDA-coated LCE film was about 2.8 cm. After an irradiation of 3 s, the PDA-coated LCE film could lift the tweezers by 0.4 cm (i.e., the length of LCE film shrunk to 2.4 cm). If the scanning time was further increased to 9 s, the tweezers could be lifted by 1.1 cm. It is noted that the weight of the film is 0.1 g, whereas the lifted pair of tweezers have a weight of 12 g. The work density of the PDA-coated LCE film could be estimated to be around 10 kJ/m^3, which is comparable to that of typical mammalian skeletal muscle (around 8 kJ/m^3).[43] More details of the demonstration are available in Movies S1 and S2 in the Supporting Information.

The temperature profile of the PDA-coated LCE film subjected to the irradiation of laser is shown in Figure 2D with the prestretch of 300%. At roughly 5.1 s, the laser was turned on and then turned off at 5.5 s. The temperature of the LCE film was the highest around the laser spot. The highest temperature in the film under the NIR laser irradiation versus time is shown in Figure 2D-i. The temperature profile of the LCE sample at 5.446 s is shown in Figure 2D-ii. It can be found that once the NIR laser irradiation was applied onto the film, the temperature was sharply increased from 22.9 to 160.2 °C within 0.4 s. The temperature was decreased to 80 °C within 1.4 s and to 30 °C within 30 s after the laser irradiation was turned off. We have repeated the same experiments multiple times for the same LCE sample. In terms of its actuation behavior, no obvious degradation of the polymer was detected. The LCE film may degrade slowly if it stays at the high temperature for longer time, which was beyond the scope of the current study.

During the testing process, the size of the laser spot was roughly 7 mm × 4 mm and the distance between the laser and the PDA-coated LCE film was around 20 cm. We believe both the actuation stress/strain and response time can be further improved if the size of the laser spot is increased to be comparable to the size of the LCE film. In addition, because both the photothermal effect and mechanical properties of LCE can be affected by the ambient temperature, the actuation performance of the PDA-coated LCE film could be also affected by the ambient temperature.

3.3. Light-Induced Fast Bending in PDA-Coated LCE Films. In addition to high actuating stress generated in the PDA-coated LCE film, large and fast deflection can also be realized in the film by NIR irradiation. As shown in Figure 3, different deformation modes of the film could be realized by adjusting the laser irradiation method. In the experiment, one end of the film was clamped and the other end was left free. Figure 3A demonstrates the large and fast deflection of a single-layer PDA-coated LCE film. After being exposed to an NIR laser spot, the PDA layer converted the light to heat locally and the temperature of LCE film was increased inhomogeneously along its thickness, which resulted in severe localized bending. It has been shown that the bending was completely reversible and the kinking position in the film could be easily controlled

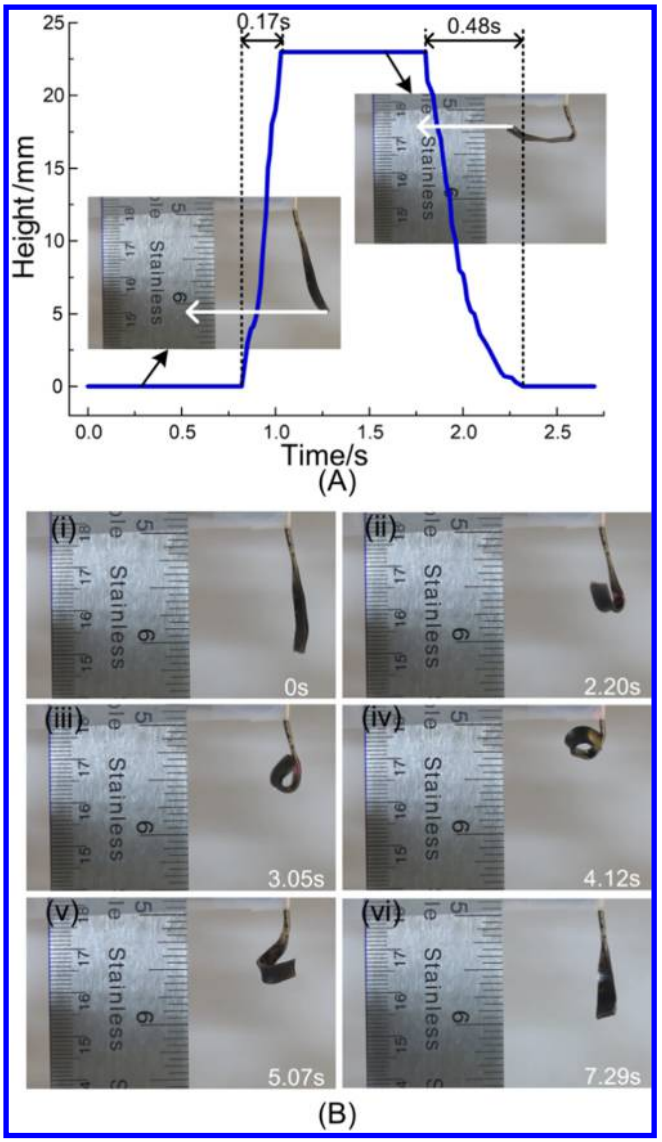

Figure 3. (A) Deflection of PDA-coated monodomain LCE film under laser irradiation at one point. (B) Rolling up of PDA-coated monodomain LCE film with light scanning on the surface of a film from bottom to top. At 4.12 s, the laser was turned off and the PDA-coated LCE film recovered back to its original flat shape within 3 s.

by varying the position of the laser spot (see Movie S3 in the Supporting Information). It has been further shown that the LCE film could bend immediately after its exposure to NIR laser. Quantitatively, the free end of the clamped LCE film could be lifted 22.5 mm within 0.17 s and recovered to the initial state within 0.48 s. The response time of the LCE film was less than 1 s, which was much shorter than that of most previously reported LCE films.[10,62] The fast response of PDA-coated LCE film may be attributed to the high energy-transferring efficiency of the PDA layer. When the laser spot was fast-scanned from the bottom to top of the film, the PDA-coated LCE film could be also rolled up as shown in Figure 3B. This was simply because the laser scanning time was shorter than the recovery time of the LCE film. More details are demonstrated in Movie S4 in the Supporting Information. The optically induced rolling up in the LCE film may find its application as a gripping mechanism for soft robots.

DOI: 10.1021/acsami.8b00639
ACS Appl. Mater. Interfaces 2018, 10, 8307−8316

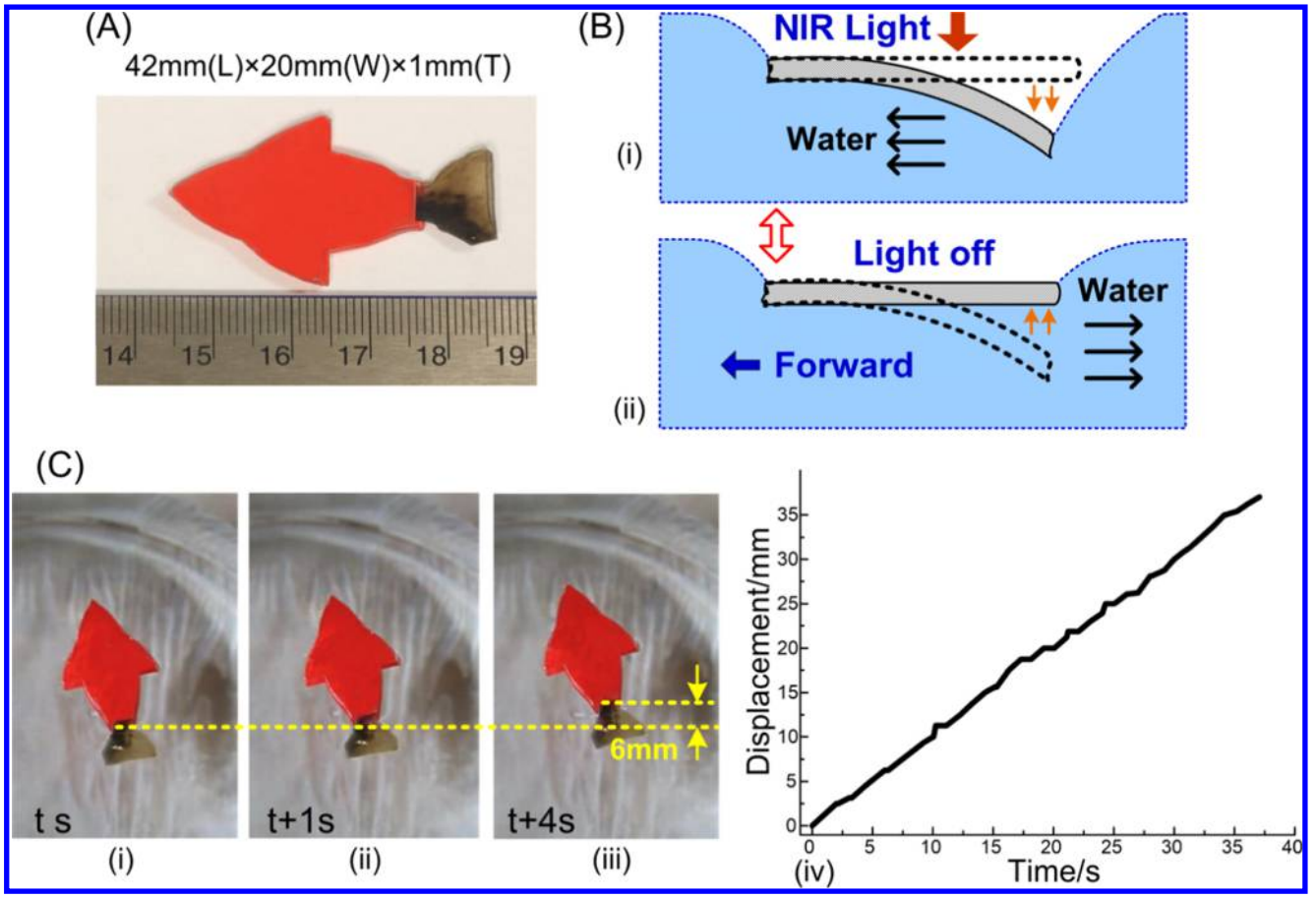

Figure 4. (A) Geometry of the designed soft robotic swimmer. (B) Schematics of the bending (i)/unbending (ii) of the caudal fin (side view) that drove the swimming of the fish near the air−water interface. (C) Measurement of the swimming distance during one swimming stroke, and the swimming distance of the swimmer as a function of time.

3.4. Light-Controlled Swimming of a Soft Robot. The rapid response of PDA-coated LCE film accompanied with large deformation and strong force generation makes it an ideal choice of "power source" to activate macroscale soft robotics and artificial muscle. Here, we designed a prototype of robotic swimmer that was able to swim near the water and air interface by performing "swimming strokes" through reversible bending and unbending motions controlled by an NIR light (see Movie S3, Supporting Information). As shown in Figure 4A, we fabricated a soft swimmer with a fish shape and 1 mm thickness. Its body and the caudal fin were made of VHB film (an adhesive film from 3 M company), which was simply adhered to PDA-coated LCE film. It is noted that although the density of the VHB (around 1.05 g/cm^3) and the PDA-coated LCE (around 2.36 g/cm^3) were larger than the density of water, the swimmer could still float on the water surface due to surface tension of water. In this design, the PDA was only coated on the bottom surface of the LCE film; thus, the artificial caudal fin can only bend downward with a merit of being guaranteed under the water interface. Otherwise, if the PDA layer was coated on the top surface of the LCE film, the film bends upward under the illumination of the laser, which may cause the film to be separated from the water, consequently leading to no interaction between the artificial tail and water. For the design of soft swimming robot, we would also like to point out that because the laser irradiation needs to transmit through the LCE film to be absorbed by the PDA coating on the bottom surface, an LCE film with too large thickness may result in the failure of swimming.

As illustrated in Figure 4B, the swimming motion was powered by the momentum exchange between the solid caudal fin and the ambient fluid. Figure 4B-i shows the tail bent downward as the surface LCE film being heated up when exposing to an NIR light. When the NIR light was turned off, as illustrated in Figure 4B-ii, the restoring elastic force quickly drove the tail to move upward and squeezed the fluid backward, which effectively generated thrust force to push the entire body forward. Moreover, as demonstrated in Movie S5, further measurements reveal that the enhanced heat dissipation in water in fact leads to a relatively gentle bending (actuation) of the caudal fin, followed by a more rapid unbending (recovery), in contrast to the quick bending and slow unbending motions observed in Figure 3A. Therefore, such asymmetric responsive behaviors of the caudal fin led to stronger momentum exchange as the tail unbent and hence further facilitated the forward swimming.

Figure 4C-i−iii shows sequential snapshots of the forward swimming motion during one swimming stroke. We have estimated that the overall net locomotion distance during each cycle was approximately 6 mm (time period 4 s). More details of the controllable continuous floating motion can be observed in Movie S6. The continuous swimming displacement as a function of time for the soft swimmer is demonstrated in Figure 4C-iv. In the experiment, the NIR irradiation was periodically turned on and off manually. Approximately, the NIR irradiation

DOI: 10.1021/acsami.8b00639
ACS Appl. Mater. Interfaces 2018, 10, 8307−8316

was kept on for 1 s and off for 2 s. From Figure 4C-iv, we can easily estimate the average speed of the swimmer to be around 1 mm/s.

Although the swimming reported here may be strongly coupled with the boundary effect,[63] it is intriguing to extend the current study to more complex fish swimming by tuning the material density to make the swimmer neutrally buoyant. To design macroscale biomimetic swimming robots (e.g., fish) with optimal performances, it then requires tightly coupled efforts in analysis and control, as well as thorough understandings of the reciprocal dynamics (flow structure, solid deformation, etc.) during fluid−structure interactions to mimic various swimming modes (undulatory or oscillatory).

It is also worthwhile to mention that while being adsorbed at the interface due to the surface tension, compared to the microscale "surfers" that are typically of microns, our swimmer had a much larger size (in centimeters). Moreover, the direction of the thermal gradient was approximately perpendicular to the swimming direction and hence the photothermal Marangoni effect was negligible in our experiments.[64,65]

Finally, we would like briefly summarize the main advantages PDA-coated LCE as artificial muscle. Compared to the actuation of LCE induced by Joule heating,[66] light-induced actuation can be remotely and more precisely controlled. One important advantage of the PDA-coated LCE developed in the study is its easy preparation and robustness, compared to the method of integrating photosensitive groups into the polymer chains of LCE (e.g., azobenzene).[67−69] Because of the unique properties of polydopamine molecules, our method can be applied to various LCEs synthesized by different methods reported in the literature. The polydopamine coating is through self-assembly process; therefore, no additional complex treatment is needed, such as vacuum evaporation, spin coating, and chemical synthesis. Moreover, it will be very easy to generate different patterns of polydopamine coating on the surface of LCE film by simply using customized masks, which can be useful to realize programmable light-induced deformation in LCE. Such programmability is hard to be realized in the optically responsive LCE doped with CNT, graphene, or carbon black.

4. CONCLUSIONS

In this study, we fabricated PDA-coated LCE film as optically driven artificial muscle. Because of the high photothermal conversion efficiency of the coated PDA layer, the fabricated elastomer film could respond to NIR light irradiation within one-tenth of a second. Furthermore, the optically induced stress or strain in the film could be significantly larger than the active stress or strain generated in mammalian skeletal muscle. We also realized different deformation modes in the film through varying the means of light illumination. To demonstrate the potential applications of the PDA-coated LCE as artificial muscle, we fabricated robotic swimmer with centimeter size that was able to swim near the water−air interface controlled by an NIR light.

■ ASSOCIATED CONTENT

Supporting Information

The Supporting Information is available free of charge on the ACS Publications website at DOI: 10.1021/acsami.8b00639.

Characterization of PDA-coated LCE film by differential scanning calorimetry (DSC) and atomic force microscopy (AFM) (Figures S1 and S2, respectively); influence of the prestretch on the LCE film (Figure S3) (PDF)

Dynamic behavior of the PDA-coated LCE film of lifting a pair of tweezers under NIR irradiation for 3 and 9 s (Movies S1 and S2, respectively); deflection of PDA-coated LCE film when exposed to a single NIR laser spot inside the environment of air and water (Movies S3 and S5, respectively); rolling up of PDA-coated LCE film through NIR laser scanning (Movie S4); light-controlled swimming of robotic swimmer based on PDA-coated LCE film (Movie S6) (AVI)(AVI)(AVI)(AVI)(AVI)(AVI)

■ AUTHOR INFORMATION

Corresponding Author

*E-mail: shqcai@ucsd.edu.

ORCID

Hongmiao Tian: 0000-0002-7377-8492

Zhijian Wang: 0000-0003-2929-8376

Jinyou Shao: 0000-0003-2525-4587

Author Contributions

#H.T. and Z.W. contributed equally to this work.

Notes

The authors declare no competing financial interest.

■ ACKNOWLEDGMENTS

H.T. acknowledges the support by China Scholarship Council (grant No. 201506285055) as a visiting scholar at University of California, San Diego, and the Fund of NSFC through grant No. 51505370. S.C. acknowledges the support from National Science Foundation through grant No. CMMI-1554212 and ONR through grant number N000141712062 (Dr. Tom McKenna). T.G. acknowledges the NSF grants DMS-1619960 and CBET-1702987.

■ REFERENCES

(1) Chen, L.; Liu, C.; Liu, K.; Meng, C.; Hu, C.; Wang, J.; Fan, S. High-Performance, Low-Voltage, and Easy-Operable Bending Actuator Based on Aligned Carbon Nanotube/Polymer Composites. *ACS Nano* **2011**, *5*, 1588−1593.

(2) Chen, L.; Weng, M.; Zhou, Z.; Zhou, Y.; Zhang, L.; Li, J.; Huang, Z.; Zhang, W.; Liu, C.; Fan, S. Large-Deformation Curling Actuators Based on Carbon Nanotube Composite: Advanced-Structure Design and Biomimetic Application. *ACS Nano* **2015**, *9*, 12189−12196.

(3) Huang, H.-W.; Sakar, M. S.; Petruska, A. J.; Pané, S.; Nelson, B. J. Soft micromachines with programmable motility and morphology. *Nat. Commun.* **2016**, *7*, No. 12263.

(4) Xu, X.; Li, H.; Zhang, Q.; Hu, H.; Zhao, Z.; Li, J.; Li, J.; Qiao, Y.; Gogotsi, Y. Self-Sensing, Ultralight, and Conductive 3D Graphene/Iron Oxide Aerogel Elastomer Deformable in a Magnetic Field. *ACS Nano* **2015**, *9*, 3969−3977.

(5) White, T. J.; Broer, D. J. Programmable and adaptive mechanics with liquid crystal polymer networks and elastomers. *Nat. Mater.* **2015**, *14*, 1087−1098.

(6) Lee, H.; Um, D.-S.; Lee, Y.; Lim, S.; Kim, H.-j.; Ko, H. Octopus-Inspired Smart Adhesive Pads for Transfer Printing of Semiconducting Nanomembranes. *Adv. Mater.* **2016**, *28*, 7457−7465.

(7) Gossweiler, G. R.; Brown, C. L.; Hewage, G. B.; Sapiro-Gheiler, E.; Trautman, W. J.; Welshofer, G. W.; Craig, S. L. Mechanochemically Active Soft Robots. *ACS Appl. Mater. Intefaces* **2015**, *7*, 22431−22435.

(8) Zhu, W.; Li, J.; Leong, Y. J.; Rozen, I.; Qu, X.; Dong, R.; Wu, Z.; Gao, W.; Chung, P. H.; Wang, J.; Chen, S. 3D-Printed Artificial Microfish. *Adv. Mater.* **2015**, *27*, 4411−4417.

DOI: 10.1021/acsami.8b00639
ACS Appl. Mater. Interfaces 2018, 10, 8307−8316

(9) Ahir, S. V.; Terentjev, E. M. Photomechanical actuation in polymer−nanotube composites. *Nat. Mater.* **2005**, *4*, 491−495.
(10) Li, C.; Liu, Y.; Lo, C.-w.; Jiang, H. Reversible white-light actuation of carbon nanotube incorporated liquid crystalline elastomer nanocomposites. *Soft Matter* **2011**, *7*, 7511−7516.
(11) Martinez, R. V.; Glavan, A. C.; Keplinger, C.; Oyetibo, A. I.; Whitesides, G. M. Soft Actuators and Robots that Are Resistant to Mechanical Damage. *Adv. Funct. Mater.* **2014**, *24*, 3003−3010.
(12) Yang, D.; Mosadegh, B.; Ainla, A.; Lee, B.; Khashai, F.; Suo, Z.; Bertoldi, K.; Whitesides, G. M. Buckling of Elastomeric Beams Enables Actuation of Soft Machines. *Adv. Mater.* **2015**, *27*, 6323−6327.
(13) Bauer, S.; Bauer-Gogonea, S.; Graz, I.; Kaltenbrunner, M.; Keplinger, C.; Schwödiauer, R. 25th Anniversary Article: A Soft Future: From Robots and Sensor Skin to Energy Harvesters. *Adv. Mater.* **2014**, *26*, 149−162.
(14) Bartlett, N. W.; Tolley, M. T.; Overvelde, J. T. B.; Weaver, J. C.; Mosadegh, B.; Bertoldi, K.; Whitesides, G. M.; Wood, R. J. A 3D-printed, functionally graded soft robot powered by combustion. *Science* **2015**, *349*, 161−165.
(15) Lekakou, C.; Elsayed, Y.; Geng, T.; Saaj, C. M. Skins and Sleeves for Soft Robotics: Inspiration from Nature and Architecture. *Adv. Eng. Mater.* **2015**, *17*, 1180−1188.
(16) Chun, K.-Y.; Kim, S. H.; Shin, M. K.; Kwon, C. H.; Park, J.; Kim, Y. T.; Spinks, G. M.; Lima, M. D.; Haines, C. S.; Baughman, R. H.; Kim, S. J. Hybrid carbon nanotube yarn artificial muscle inspired by spider dragline silk. *Nat. Commun.* **2014**, *5*, No. 3322.
(17) Li, W.; Wang, J.; Ren, J.; Qu, X. 3D Graphene Oxide-Polymer Hydrogel: Near-Infrared Light-Triggered Active Scaffold for Reversible Cell Capture and On-Demand Release. *Adv. Mater.* **2013**, *25*, 6737−6743.
(18) Lv, J.-a.; Liu, Y.; Wei, J.; Chen, E.; Qin, L.; Yu, Y. Photocontrol of fluid slugs in liquid crystal polymer microactuators. *Nature* **2016**, *537*, 179−184.
(19) Loomis, J.; Fan, X.; Khosravi, F.; Xu, P.; Fletcher, M.; Cohn, R. W.; Panchapakesan, B. Graphene/elastomer composite-based photothermal nanopositioners. *Sci. Rep.* **2013**, *3*, No. 1900.
(20) Feng, Y.; Qin, M.; Guo, H.; Yoshino, K.; Feng, W. Infrared-Actuated Recovery of Polyurethane Filled by Reduced Graphene Oxide/Carbon Nanotube Hybrids with High Energy Density. *ACS Appl. Mater. Interfaces* **2013**, *5*, 10882−10888.
(21) Yu, L.; Yu, H. Light-Powered Tumbler Movement of Graphene Oxide/Polymer Nanocomposites. *ACS Appl. Mater. Interfaces* **2015**, *7*, 3834−3839.
(22) Koerner, H.; Price, G.; Pearce, N. A.; Alexander, M.; Vaia, R. A. Remotely actuated polymer nanocomposites—stress-recovery of carbon-nanotube-filled thermoplastic elastomers. *Nat. Mater.* **2004**, *3*, 115−120.
(23) Palffy-Muhoray, P. The diverse world of liquid crystals. *Phys. Today* **2007**, *60*, 54−60.
(24) Yu, L.; Cheng, Z.; Dong, Z.; Zhang, Y.; Yu, H. Photomechanical response of polymer-dispersed liquid crystals/graphene oxide nanocomposites. *J. Mater. Chem. C.* **2014**, *2*, 8501−8506.
(25) White, T. J. Light to work transduction and shape memory in glassy, photoresponsive macromolecular systems: Trends and opportunities. *J. Polym. Sci., Part B: Polym. Phys.* **2012**, *50*, 877−880.
(26) Jiang, W.; Niu, D.; Liu, H.; Wang, C.; Zhao, T.; Yin, L.; Shi, Y.; Chen, B.; Ding, Y.; Lu, B. Photoresponsive Soft-Robotic Platform: Biomimetic Fabrication and Remote Actuation. *Adv. Funct. Mater.* **2014**, *24*, 7598−7604.
(27) Tai, Y.; Lubineau, G.; Yang, Z. Light-Activated Rapid-Response Polyvinylidene-Fluoride-Based Flexible Films. *Adv. Mater.* **2016**, *28*, 4665−4670.
(28) Zhang, X.; Yu, Z.; Wang, C.; Zarrouk, D.; Seo, J.-W. T.; Cheng, J. C.; Buchan, A. D.; Takei, K.; Zhao, Y.; Ager, J. W.; Zhang, J.; Hettick, M.; Hersam, M. C.; Pisano, A. P.; Fearing, R. S.; Javey, A. Photoactuators and motors based on carbon nanotubes with selective chirality distributions. *Nat. Commun.* **2014**, *5*, No. 2983.
(29) ter Schiphorst, J.; Coleman, S.; Stumpel, J. E.; Azouz, A. B.; Diamond, D.; Schenning, A. P. H. J. Molecular Design of Light-Responsive Hydrogels, For in Situ Generation of Fast and Reversible Valves for Microfluidic Applications. *Chem. Mater.* **2015**, *27*, 5925−5931.
(30) Kim, D.; Lee, H. S.; Yoon, J. Highly bendable bilayer-type photo-actuators comprising of reduced graphene oxide dispersed in hydrogels. *Sci. Rep.* **2016**, *6*, No. 20921.
(31) Meng, H.; Li, G. A review of stimuli-responsive shape memory polymer composites. *Polymer* **2013**, *54*, 2199−2221.
(32) Hager, M. D.; Bode, S.; Weber, C.; Schubert, U. S. Shape memory polymers: Past, present and future developments. *Prog. Polym. Sci.* **2015**, *49*−*50*, 3−33.
(33) Palagi, S.; Mark, A. G.; Reigh, S. Y.; Melde, K.; Qiu, T.; Zeng, H.; Parmeggiani, C.; Martella, D.; Sanchez-Castillo, A.; Kapernaum, N.; Giesselmann, F.; Wiersma, D. S.; Lauga, E.; Fischer, P. Structured light enables biomimetic swimming and versatile locomotion of photoresponsive soft microrobots. *Nat. Mater.* **2016**, *15*, 647−653.
(34) Li, C.; Liu, Y.; Huang, X.; Jiang, H. Direct Sun-Driven Artificial Heliotropism for Solar Energy Harvesting Based on a Photo-Thermomechanical Liquid-Crystal Elastomer Nanocomposite. *Adv. Funct. Mater.* **2012**, *22*, 5166−5174.
(35) Kamenjicki, M.; Lednev, I. K.; Asher, S. A. Photoresponsive Azobenzene Photonic Crystals. *J. Phys. Chem. B* **2004**, *108*, 12637−12639.
(36) Satoh, T.; Sumaru, K.; Takagi, T.; Kanamori, T. Fast-reversible light-driven hydrogels consisting of spirobenzopyran-functionalized poly(N-isopropylacrylamide). *Soft Matter* **2011**, *7*, 8030−8034.
(37) Ziółkowski, B.; Florea, L.; Theobald, J.; Benito-Lopez, F.; Diamond, D. Porous self-protonating spiropyran-based NIPAAm gels with improved reswelling kinetics. *J. Mater. Sci.* **2016**, *51*, 1392−1399.
(38) Sershen, S. R.; Mensing, G. A.; Ng, M.; Halas, N. J.; Beebe, D. J.; West, J. L. Independent Optical Control of Microfluidic Valves Formed from Optomechanically Responsive Nanocomposite Hydrogels. *Adv. Mater.* **2005**, *17*, 1366−1368.
(39) Lee, E.; Kim, D.; Kim, H.; Yoon, J. Photothermally driven fast responding photo-actuators fabricated with comb-type hydrogels and magnetite nanoparticles. *Sci. Rep.* **2015**, *5*, No. 15124.
(40) Zhou, Y.; Hauser, A. W.; Bende, N. P.; Kuzyk, M. G.; Hayward, R. C. Waveguiding Microactuators Based on a Photothermally Responsive Nanocomposite Hydrogel. *Adv. Funct. Mater.* **2016**, *26*, 5447−5452.
(41) Lendlein, A.; Jiang, H.; Jünger, O.; Langer, R. Light-induced shape-memory polymers. *Nature* **2005**, *434*, 879−882.
(42) Rochette, J. M.; Ashby, V. S. Photoresponsive Polyesters for Tailorable Shape Memory Biomaterials. *Macromolecules* **2013**, *46*, 2134−2140.
(43) Camacho-Lopez, M.; Finkelmann, H.; Palffy-Muhoray, P.; Shelley, M. Fast liquid-crystal elastomer swims into the dark. *Nat. Mater.* **2004**, *3*, 307−310.
(44) Wie, J. J.; Shankar, M. R.; White, T. J. Photomotility of polymers. *Nat. Commun.* **2016**, *7*, No. 13260.
(45) Lu, X.; Guo, S.; Tong, X.; Xia, H.; Zhao, Y. Tunable Photocontrolled Motions Using Stored Strain Energy in Malleable Azobenzene Liquid Crystalline Polymer Actuators. *Adv. Mater.* **2017**, *29*, No. 1606467.
(46) Liu, Y.; Xu, B.; Sun, S.; Wei, J.; Wu, L.; Yu, Y. Humidity- and Photo-Induced Mechanical Actuation of Cross-Linked Liquid Crystal Polymers. *Adv. Mater.* **2017**, *29*, No. 1604792.
(47) Ikeda, T.; Mamiya, J.-i.; Yu, Y. Photomechanics of liquid-crystalline elastomers and other polymers. *Angew. Chem., Int. Ed.* **2007**, *46*, 506−528.
(48) Huang, C.; Lv, J.-a.; Tian, X.; Wang, Y.; Yu, Y.; Liu, J. Miniaturized Swimming Soft Robot with Complex Movement Actuated and Controlled by Remote Light Signals. *Sci. Rep.* **2015**, *5*, No. 17414.
(49) Marshall, J. E.; Ji, Y.; Torras, N.; Zinoviev, K.; Terentjev, E. M. Carbon-nanotube sensitized nematic elastomer composites for IR-visible photo-actuation. *Soft Matter* **2012**, *8*, 1570−1574.
(50) Liu, X.; Wei, R.; Hoang, P. T.; Wang, X.; Liu, T.; Keller, P. Reversible and Rapid Laser Actuation of Liquid Crystalline Elastomer

DOI: 10.1021/acsami.8b00639
ACS Appl. Mater. Interfaces 2018, 10, 8307−8316

Micropillars with Inclusion of Gold Nanoparticles. *Adv. Funct. Mater.* **2015**, *25*, 3022−3032.
(51) Yang, H.; Liu, J.-J.; Wang, Z.-F.; Guo, L.-X.; Keller, P.; Lin, B.-P.; Sun, Y.; Zhang, X.-Q. Near-infrared-responsive gold nanorod/liquid crystalline elastomer composites prepared by sequential thiol-click chemistry. *Chem. Commun.* **2015**, *51*, 12126−12129.
(52) Liu, Y.; Ai, K.; Liu, J.; Deng, M.; He, Y.; Lu, L. Dopamine−Melanin Colloidal Nanospheres: An Efficient Near-Infrared Photothermal Therapeutic Agent for In Vivo Cancer Therapy. *Adv. Mater.* **2013**, *25*, 1353−1359.
(53) Li, Z.; Yang, Y.; Wang, Z.; Zhang, X.; Chen, Q.; Qian, X.; Liu, N.; Wei, Y.; Ji, Y. Polydopamine nanoparticles doped in liquid crystal elastomers for producing dynamic 3D structures. *J. Mater. Chem. A* **2017**, *5*, 6740−6746.
(54) Li, Z.; Zhang, X.; Wang, S.; Yang, Y.; Qin, B.; Wang, K.; Xie, T.; Wei, Y.; Ji, Y. Polydopamine coated shape memory polymer: enabling light triggered shape recovery, light controlled shape reprogramming and surface functionalization. *Chem. Sci.* **2016**, *7*, 4741−4747.
(55) Lee, H.; Dellatore, S. M.; Miller, W. M.; Messersmith, P. B. Mussel-inspired surface chemistry for multifunctional coatings. *Science* **2007**, *318*, 426−430.
(56) Frick, C. P.; Merkel, D. R.; Laursen, C. M.; Brinckmann, S. A.; Yakacki, C. M. Copper-Coated Liquid-Crystalline Elastomer via Bioinspired Polydopamine Adhesion and Electroless Deposition. *Macromol. Rapid Commun.* **2016**, *37*, 1912−1917.
(57) Yakacki, C. M.; Saed, M.; Nair, D. P.; Gong, T.; Reed, S. M.; Bowman, C. N. Tailorable and programmable liquid-crystalline elastomers using a two-stage thiol−acrylate reaction. *RSC Adv.* **2015**, *5*, 18997−19001.
(58) Saed, M. O.; Torbati, A. H.; Nair, D. P.; Yakacki, C. M. Synthesis of Programmable Main-chain Liquid-crystalline Elastomers Using a Two-stage Thiol-acrylate Reaction. *J. Visualized Exp.* **2016**, *107*, No. e53546.
(59) Baginska, M.; Blaiszik, B. J.; Rajh, T.; Sottos, N. R.; White, S. R. Enhanced autonomic shutdown of Li-ion batteries by polydopamine coated polyethylene microspheres. *J. Power Sources* **2014**, *269*, 735−739.
(60) Madden, J. D. W.; Vandesteeg, N. A.; Anquetil, P. A.; Madden, P. G. A.; Takshi, A.; Pytel, R. Z.; Lafontaine, S. R.; Wieringa, P. A.; Hunter, I. W. Artificial Muscle Technology: Physical Principles and Naval Prospects. *IEEE J. Oceanic Eng.* **2004**, *29*, 706−728.
(61) Vallbo, A. B. Muscle spindle response at the onset of isometric voluntary contractions in man. Time difference between fusimotor and skeletomotor effects. *J. Physiol.* **1971**, *218*, 405−431.
(62) Takashima, Y.; Hatanaka, S.; Otsubo, M.; Nakahata, M.; Kakuta, T.; Hashidzume, A.; Yamaguchi, H.; Harada, A. Expansion−contraction of photoresponsive artificial muscle regulated by host−guest interactions. *Nat. Commun.* **2012**, *3*, No. 1270.
(63) Childress, S.; Hosoi, A.; Schultz, W. W.; Wang, J. *Natural Locomotion in Fluids and on Surfaces: Swimming, Flying, and Sliding*; Springer Science & Business Media: New York, 2012.
(64) Anderson, J. L. Colloid transport by interfacial forces. *Annu. Rev. Fluid Mech.* **1989**, *21*, 61−99.
(65) Würger, A. Thermally driven Marangoni surfers. *J. Fluid Mech.* **2014**, *752*, 589−601.
(66) Yuan, C.; Roach, D. J.; Dunn, C. K.; Mu, Q.; Kuang, X.; Yakacki, C. M.; Wang, T. J.; Yu, K.; Qi, H. J. 3D printed reversible shape changing soft actuators assisted by liquid crystal elastomers. *Soft Matter* **2017**, *13*, 5558−5568.
(67) White, T. J.; Tabiryan, N. V.; Serak, S. V.; Hrozhyk, U. A.; Tondiglia, V. P.; Koerner, H.; Vaia, R. A.; Bunning, T. J. A high frequency photodriven polymer oscillator. *Soft Matter* **2008**, *4*, 1796−1798.
(68) Lee, K. M.; Koerner, H.; Vaia, R. A.; Bunning, T. J.; White, T. J. Light-activated shape memory of glassy, azobenzene liquid crystalline polymer networks. *Soft Matter* **2011**, *7*, 4318−4324.
(69) Gelebart, A. H.; Mulder, D. J.; Varga, M.; Konya, A.; Vantomme, G.; Meijer, E. W.; Selinger, R. L. B.; Broer, D. J. Making waves in a photoactive polymer film. *Nature* **2017**, *546*, 632−636.

DOI: 10.1021/acsami.8b00639
ACS Appl. Mater. Interfaces 2018, 10, 8307−8316